BMC Cancer

RESEARCH

Open Access

SIRT7 affects the proliferation and apoptosis of papillary thyroid cancer cells by desuccinylation of LATS1

Qinghua Li[1] and Gang Pu[1*]

Abstract

Background Papillary thyroid cancer (PTC) is one of the malignant tumors with rapidly increasing morbidity and mortality. Sirtuin 7 (SIRT7) is a desuccinylase that is involved in tumorigenesis. The activation of large tumor suppressor 1 (LATS1) can effectively suppress tumorigenesis in multiple tumors and can be affected by SIRT7. This study aimed to explore the role and mechanism of SIRT7 in PTC progression.

Methods The RNA and protein levels were detected by quantitative real-time PCR (qPCR) and western blot, respectively. Cell proliferation was measured by cell counting kit-8 and colony formation. The apoptosis of PTC cells was analyzed by flow cytometry and Live/dead cell staining. The interaction between proteins was detected by co-immunoprecipitation.

Results The results showed that SIRT7 was highly expressed in PTC tissues and cells. Functional studies showed that knockdown of SIRT7 inhibited the proliferation and induced apoptosis of PTC cells. Mechanistically, SIRT7 could directly interact with LATS1 and reduce the stability of the LATS1 protein. Later, rescue experiments suggested that LATS1 silencing reversed the effect of SIRT7 knockdown on PTC cell growth and apoptosis. In addition, SIRT7 promoted tumor growth in vivo.

Conclusion Taken together, silencing of SIRT7 promotes the succinylation of LATS1 to enhance LATS1 stability, thus inhibiting the progression of PTC. Therefore, SIRT7 and LATS1 may become novel and potential therapeutic targets for PTC.

Keywords Papillary thyroid cancer, SIRT7, Succinylation, LATS1, Apoptosis

*Correspondence:
Gang Pu
13624420055@163.com
[1]Department of Thyroid Surgery, Affiliated Hospital of Beihua University, No. 12, Jiefang Middle Road, Chuanying District, Jilin City, Jilin Province 132001, China

Introduction

Papillary thyroid cancer (PTC) is one of the most common malignant tumors of the endocrine system, accounting for about 90% of all follicular-derived well-differentiated thyroid cancers (TC) [1]. Although PTC growth is slow and the overall prognosis is good, most patients with PTC have cervical lymph node metastasis at the time of diagnosis [2]. In addition, a small percentage of tumors exhibit more aggressive heterogeneity with higher rates of recurrence and metastasis [3]. Therefore, it is of great significance to further explore the functional genes related to the occurrence and development of PTC and find new potential diagnostic and therapeutic targets.

Succinylation is a post-translational modification of proteins that is the process by which succinyl donors covalently bind succinyl groups to lysine residues by enzymatic or non-enzymatic methods [4]. It is usually regulated by desuccinylases such as sirtuin 5 (SIRT5) and sirtuin 7 (SIRT7) in eukaryotes [5]. Abnormal succinylation can affect the development of several diseases, such as tumors, cardiometabolic diseases, liver metabolic diseases, and nervous system diseases [6]. Growing evidence has demonstrated that various cancers can be promoted or inhibited by modulating the level of succinylation at substrate targets [7–9]. Succinylation can promote the occurrence of gastric cancer, breast cancer, renal clear cell carcinoma, and glioma, and has a tumor-suppressive effect on lung cancer, liver cancer, and osteosarcoma [10]. However, relatively few studies have investigated the role of succinylation in PTC. Existing research shows that succinylation can affect thyroid hormone synthesis, and regulation of this post-translational modification can inhibit apoptosis and migration of TC cells [11]. However, the specific regulatory mechanism of succinylation in PTC is still unclear.

SIRT7, as an NAD+-dependent histone desuccinylase, is a member of the sirtuin (SIRT) family, which is involved in gene regulation, genome stabilization, aging, tumorigenesis, and other processes [12]. The dysregulation in SIRT7 disrupts metabolic homeostasis, accelerates aging, and increases the risk of age-related diseases, including cardiovascular, neurodegenerative, kidney, lung, and inflammatory diseases, and cancers [13]. Evidence suggests that SIRT7 is highly expressed in different types of cancer [14]. It is worth noting that SIRT7 promotes the proliferation and migration of anaplastic TC cells by regulating the desuccinylation of KIF23 [15]. SIRT7 promotes thyroid tumorigenesis through phosphorylation and activation of Akt and p70S6K1 via the modulation of the DBC1/SIRT1 axis [16]. However, the molecular mechanism of SIRT7-mediated succinylation in PTC remains not fully elucidated and requires further study.

Large tumor suppressor 1 (LATS1) has the function of modulating many carcinogenic or tumor suppressor effectors, including the Aurora mitotic kinase family, the canonical Hippo effectors YAP/TAZ, and the tumor suppressive transcription factor p53 [17]. A study has shown that overexpression of LATS1 inhibits nuclear translocation of YAP in TC cell lines, thereby activating the Hippo signaling pathway to inhibit proliferation, migration, and invasion and promote apoptosis of TC cells [18]. Interestingly, SIRT7 promotes deacetylation of DNA damage-binding protein 1, leading to the accumulation or activation of LATS1 and p73, which contribute to actinobacillin-D and 5-fluorouracil-induced apoptosis [19].

Given the relationship between SIRT7 and LATS1, in this study, we aimed to investigate the effect of SIRT7 on PTC progression and whether LATS1 was involved in SIRT7-mediated succinylation in the PTC. This study may provide a new strategy and research direction for the treatment of PTC.

Materials and methods

Bioinformatic analysis

The association genes of SIRT7 in PTC were predicted by the LinkedOmics database (https://www.linkedomics.org/login.php).

The succinylation modification sites in LATS1 were predicted by the GPSuc website (http://kurata14.bio.kyutech.ac.jp/GPSuc/).

Clinical sample collection

Thirty-two PTC tissue specimens and corresponding adjacent non-tumor tissues from patients with PTC were collected and stored in liquid nitrogen for use. All tissue samples were verified by pathological examination. Patients were enrolled in this study after signing written informed consent, and this study was approved by the Ethics Committee of Affiliated Hospital of Beihua University.

Cell culture

Human normal thyroid cell lines Nthyori-3 and PTC cell lines (TPC-1 and KTC-1) were purchased from the Chinese Academy of Sciences (Shanghai, China). All cell lines were routinely cultured in Dulbecco's modified Eagle's medium (DMEM; ThermoFisher, Waltham, MA, USA) containing 10% fetal bovine serum (FBS; Biosera, Nuaille, France), 100 U/mL penicillin, and 100 mg/mL streptomycin at 37℃ with 5% CO_2. The culture medium was changed every 2 ~ 3 days. The cells in the logarithmic growth phase were used.

Cell transfection

Short hairpin (sh) RNA targeting SIRT7 (shSIRT7), shRNA targeting LATS1 (sh LATS1), and shRNA

negative control (shNC) were synthesized by Genepharma (Shanghai, China). LATS1 site-directed mutant plasmids (K6R, K589R, and K652R) were generated using the QuickChange II site-directed mutagenesis kit (Applied BioSystems, Carlsbad, CA, USA) according to the manufacturer's instructions. The cells (6×10^4 cells/mL) in the logarithmic growth stage were collected and seeded in six-well plates at the density of 2 mL/well. Transfection was conducted in PTC cells using Lipofectamine 2000 (Invitrogen, Carlsbad, CA, USA) when the cell confluence reached 85%.

Quantitative real-time PCR (q-PCR)

Total RNA was separated and extracted from tissues and cell lines using Trizol reagent (Invitrogen) according to the manufacturer's instructions, and RNA concentration was measured. The Hi-Fi cDNA synthesis kit (Abcam, Cambridge, MA, UK) reversely transcribed 1 μg of total RNA into cDNA. Primers were synthesized by Sangon Biotech (Shanghai, China). The mRNA levels were measured by q-PCR in a 20 μl reaction system containing specific primers and SYBR Green Master Mix (Takara, Dalian, China) according to the manufacturer's protocols on the CFX96 Real-Time PCR detection system (Bio-Rad, Hercules, CA, USA). The amplification process was performed as follows: pre-denaturation at 95℃ for 5 min, denaturation at 95℃ for 10 s, annealing at 60℃ for 20 s, and then extension at 72℃ for 30 s, for 40 cycles. A melting curve of each amplicon was determined to verify its specificity. With GAPDH as the internal control, the relative mRNA levels were measured by a $2^{-\Delta\Delta Ct}$ method in each group.

Cell viability

Cell viability was assessed using a cell-counting kit-8 (CCK-8; Solarbio, Beijing, China) after transfection for 48 h. PTC cells were seeded to 96-well plates at the density of 1×10^3 cells/well and cultured in 200 μl 10% FBS/DMEM. After 0, 24, 48, and 72 h of inoculation, CCK-8 reagent was added to the medium and continued to culture for 2 h. The absorbance at 450 nm in each period was measured by a microplate reader (BMG Labtech, Offenburg, Germany).

Colony formation assay

PTC cells (2×10^5 cells/well) were digested and seeded into 6-well plates and transfected with plasmids after adherence. After 48 h, the cells of the logarithmic growth phase were collected and counted using cell counting plates, and about 400 cells were inoculated per well. After 14 days, the cells were fixed in 4% paraformaldehyde, stained with crystal violet (Beyotime Biotechnology, Shanghai, China), and counted.

Flow cytometry assay

The apoptosis levels of PTC cells were evaluated using the FITC-Annexin V/ propidium iodide (PI) apoptosis detection kit (Keygen Biotech, Jiangsu, China) according to the manufacturer's instructions. In short, 195 μl cell suspension (5×10^5 cells) was incubated with 5 μl FITC-Annexin V and 10 μl PI at room temperature for 15 min in the dark. After 3 times washing with PBS, a flow cytometer (BD Biosciences, San Jose, CA, USA) was used to evaluate the apoptosis percentage of PTC cells.

Live/dead cell staining

The live/dead cell staining assay using Calcein-AM (CA) and Propidium Iodide (PI) was performed to visualize apoptosis cells and live cells of PTC under various treatment conditions. Briefly, PTC cells were incubated with a staining solution containing 2 μM Calcein-AM and 5 μM PI in PBS for 20 min at 37 °C in the dark. Following incubation, cells were gently washed with PBS to eliminate unbound dyes. The stained cells were immediately visualized under a fluorescence microscope, where live cells exhibited green fluorescence due to Calcein-AM staining, while dead cells displayed red fluorescence from PI incorporation.

Co-immunoprecipitation (IP) assay

Transfected cells were harvested and lysed in ice-cold IP lysis buffer (containing protease and phosphatase inhibitors) using gentle agitation. Lysates were centrifuged to remove debris. Next, cleared lysates were incubated overnight at 4 °C with anti-Flag magnetic beads to pull down Flag-SIRT7 along with any interacting proteins. Control samples included beads incubated with lysate from cells expressing HA-LATS1 alone to assess nonspecific binding. Then, beads were washed extensively with lysis buffer to remove unbound proteins. Finally, interacting proteins were eluted using Flag peptide or denaturing conditions, depending on downstream analysis requirements. Eluates were subjected to SDS-PAGE and transferred to PVDF membranes for western blot analysis. In IgG, the light chain is one of the two smaller polypeptide chains that make up an antibody.

Protein stability assessment

To explore the protein stability of LATS1, the cells were treated with cycloheximide (CHX, 100 μg/mL, MedChemExpress, Monmouth Junction, NJ, USA), and the protein level of LATS1 at different time points (0, 8, 16, and 24 h) was detected.

Western blot

The lysis buffer was used to extract the total protein from PTC tissues or cells. After the protein concentration was determined by the BCA protein assay kit (Abcam),

50 μg of protein was separated by a 10% SDS-PAGE and then transferred to the PVDF membrane. The PVDF membrane was blocked with 5% skim milk at 37 °C for 2 h and then incubated overnight at 4 °C with the following primary antibodies: Anti-Succinyllysine (1: 500, PTM-401, PTMBIO, Hangzhou, China), SIRT7 (1: 200, ab259968, Abcam), LATS1 (1: 200, ab243656, Abcam), and β-actin (1: 200, ab8226, Abcam). The membrane was washed 3 times with TBST, 10 min each time. Then, the secondary antibody (1: 1000, AF008, Novus, Shanghai, China) was incubated for 2 h at room temperature, and the membrane was washed by TBST for 3 times, 10 min each time. Finally, band signals were visualized using an enhanced chemiluminescence solution (Thermo Fisher Scientific, Monmouth Junction, NJ, USA) and exposed in a ChemiDocTM XRSC system (Bio-Rad).

Animal study

The BALB/c nude mice (male, 6-week-old) were purchased from Charles River Experimental Animal Technology (Beijing, China) and were fed at 20–26 °C and humidity of 40–60% in a 12 h light/dark cycles condition. They were randomly divided into two groups, with six mice in each group. shNC and shSIRT7 plasmids were transfected into TPC-1 cells, respectively. The mice in the shSIRT7 group were subcutaneously injected with sh-SIRT7 transfected TPC-1 cells at the density of 5×10^6 cells, and the shNC group mice were injected with sh-NC transfected TPC-1 cells in the same way and location as the shSIRT7 group mice. Tumor volume was assessed with vernier calipers a week after injection, measured weekly for continuous four weeks, and calculated using the formula: volume (mm^3) = 0.5 × length × width^2. After four weeks, all mice were euthanized with an intraperitoneal injection of 3% pentobarbital sodium (Sigma, Germany). The tumors were dislocated, collected, and weighed. This study was approved by the Ethics Committee of Affiliated Hospital of Beihua University. All animal experiments should comply with the ARRIVE guidelines. All methods were carried out in accordance with relevant guidelines and regulations.

Hematoxylin and Eosin (HE) staining

A small piece of tumor tissue was quickly taken from the killed mice and was fixed with 4% paraformaldehyde for 24 h. The tissues were dehydrated with ethanol, embedded in paraffin, and then cut into sections with a thickness of 4 μm for use. After routine dewaxing, sections were stained with hematoxylin staining solution for 3 min and washed with water for 1 min. Then, the sections were transferred to the color separation solution for about 1 min and washed with water for 1 min. Sections were stained with eosin solution for 2 min and then rinsed with tap water for 5 min. Next, the slices are dehydrated, dried, and sealed with neutral glue. Finally, an optical microscope was used to photo, with 6 different fields of view selected for each image.

Immunohistochemistry (IHC) analysis

Paraffin-embedded tumor tissues were cut into sections, dewaxed, rehydrated, and treated with 3% H_2O_2. After treating with 10 mM citrate buffer (pH 6.0) and heating to 95℃, normal goat serum was used to block the sections at room temperature for 30 min. The sections were incubated with the primary antibody against LATS1 at 4 °C overnight and incubated with the secondary antibody at 37 °C for 1 h. The results were observed under a light microscope (Olympus, Tokyo, Japan).

Statistical analysis

Statistical analyses were conducted with GraphPad Prism 8.3 software (GraphPad Software, USA). All data obtained from at least three independent experiments were shown using mean ± standard deviation (SD). Student's t-test was employed to analyze the differences between the two groups. Differences among multiple groups were analyzed by one-way ANOVA followed by Tukey's post hoc test. The diagnosis value of SIRT7 was evaluated using the receiver operator characteristic (ROC) curve. The correlation of SIRT7 and LATS1 expression was analyzed using the Pearson correlation coefficient. P values < 0.05 were considered to be statistically significant.

Results

SIRT7 is highly expressed in PTC

To investigate the biological function of SIRT7 in PTC, we detected SIRT7 expression in PTC tissues and corresponding adjacent normal tissues. As shown in Fig. 1A, the relative expression of SIRT7 was increased in PTC tissues compared to the normal tissues by q-PCR. Likewise, the results of western blotting show that SIRT7 expression was upregulated in PTC tissues (Fig. 1B). Next, the diagnosis value of SIRT7 was evaluated using the ROC curve. The area under the curve (AUC) value was 0.9507 (Fig. 1C), suggesting that SIRT7 serves as a valuable diagnostic biomarker of PTC. Next, SIRT7 expression was detected in normal thyroid cell line Nthyori-3 and PTC cell lines TPC-1 and KTC-1. It was disclosed by q-PCR detection that the SIRT7 was overtly elevated in TPC-1 and KTC-1 cells (Fig. 1D). Consistently, the protein expression level of SIRT7 in PTC cell lines was much higher than that in the Nthyori-3 group (Fig. 1E). These results indicated that SIRT7 is highly expressed in PTC.

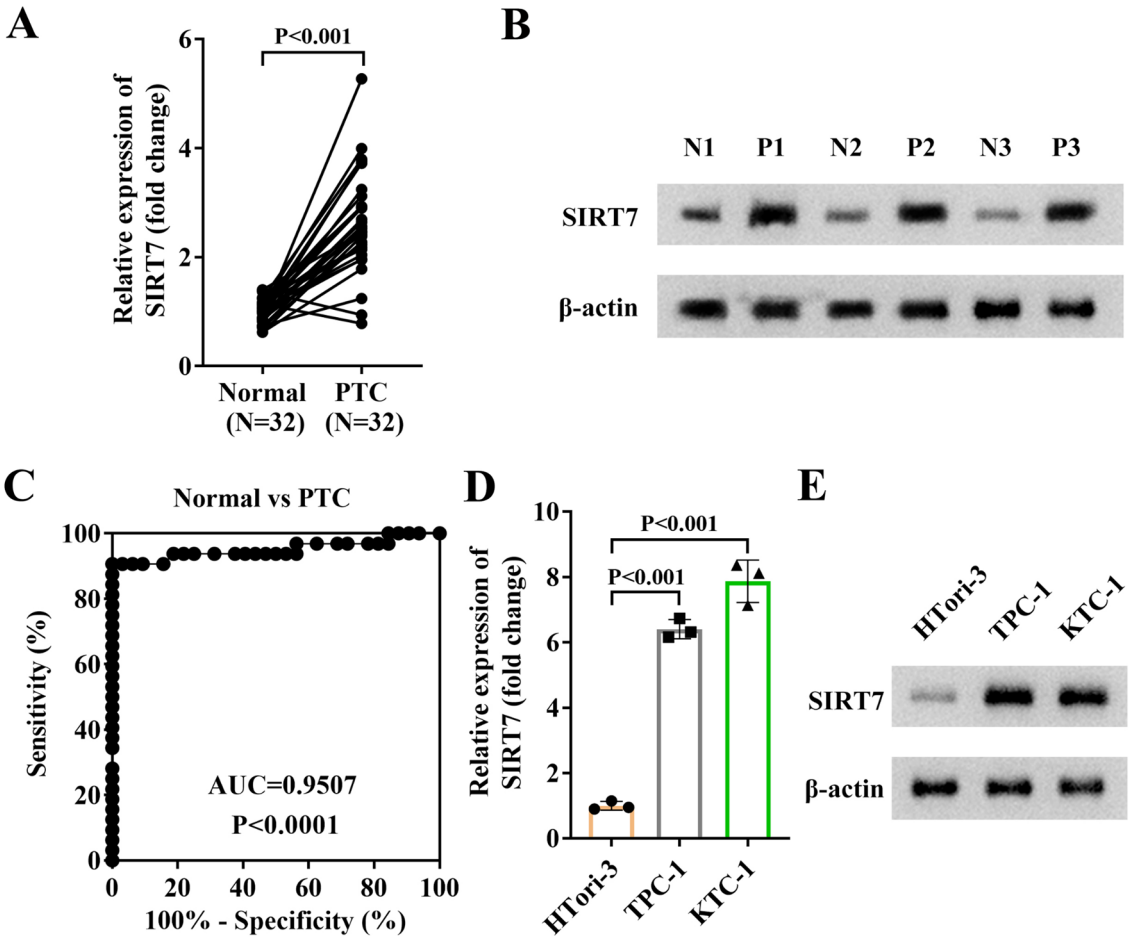

Fig. 1 SIRT7 is highly expressed in PTC. (**A**) SIRT7 expression in PTC ($n=32$) and normal ($n=32$) tissues was measured using qPCR. (**B**) The protein levels of SIRT7 were measured by western blot. (**C**) The diagnosis value of SIRT7 expression in PTC was determined using ROC curve analysis. (**D**) SIRT7 expression in normal thyroid cell line Nthyori-3 and PTC cell lines (TPC-1 and KTC-1) was measured using qPCR. (**E**) The protein levels of SIRT7 in cells were measured by western blot. All data are expressed as the means ± SD. ($n=3$ independent experiments)

Silencing of SIRT7 inhibits proliferation and promotes apoptosis of PTC cells

To further verify the role of SIRT7 in PTC, shSIRT7 and shNC were transfected into TPC-1 and KTC-1 cells. The results of q-PCR and western blot showed that SIRT7 expression was inhibited by transfecting three different shRNA interference sequences targeting the SIRT7 gene into PTC cell lines (Fig. 2A and B). Subsequently, we selected the shSIRT7 1# plasmid for post-experiments. Silencing of SIRT7 inhibited cell viability and colonies, suggesting cell proliferation was suppressed by SIRT7 silence (Fig. 2C and D). Likewise, data obtained from the flow cytometry suggested that the apoptosis rate of TPC-1 and KTC-1 cells was increased by silencing of OGT (Fig. 2E). The results of live/dead experiments further supported the above results (Fig. 2F). These data proved that SIRT7 knockdown significantly inhibits the proliferation and induces apoptosis of PTC cells.

SIRT7 regulates LATS1 by succinylation modification

Next, to explore the regulatory mechanisms of SIRT7 in PTC, we used the LinkedOmics database to predict SIRT7-correlated genes in PTC (Fig. 3A). Then, we screened the five most correlated genes, which were ATE1, WWTR1, PJA2, LATS1, and MID2. The q-PCR analysis demonstrated a remarkable augment of LATS1 expression after SIRT7 silencing in both TPC-1 and KTC-1 cells (Fig. 3B and C). After this, we found that the mRNA level and protein expression of LATS1 in PTC tissues was dramatically decreased compared with normal para-cancerous tissues (Fig. 3D and E). Later, we did the correlation analysis of SIRT7 and LATS1 and found that the relationship between them was negative (Fig. 3F). Consistently, the result of q-PCR and western blotting showed that the expression of LATS1 was down-regulated in PTC cell lines (Fig. 3G and H). Co-IP assay was performed to verify that SIRT7 directly interacted with LATS1 in TPC-1 cells (Fig. 3I). Next, three succinylation

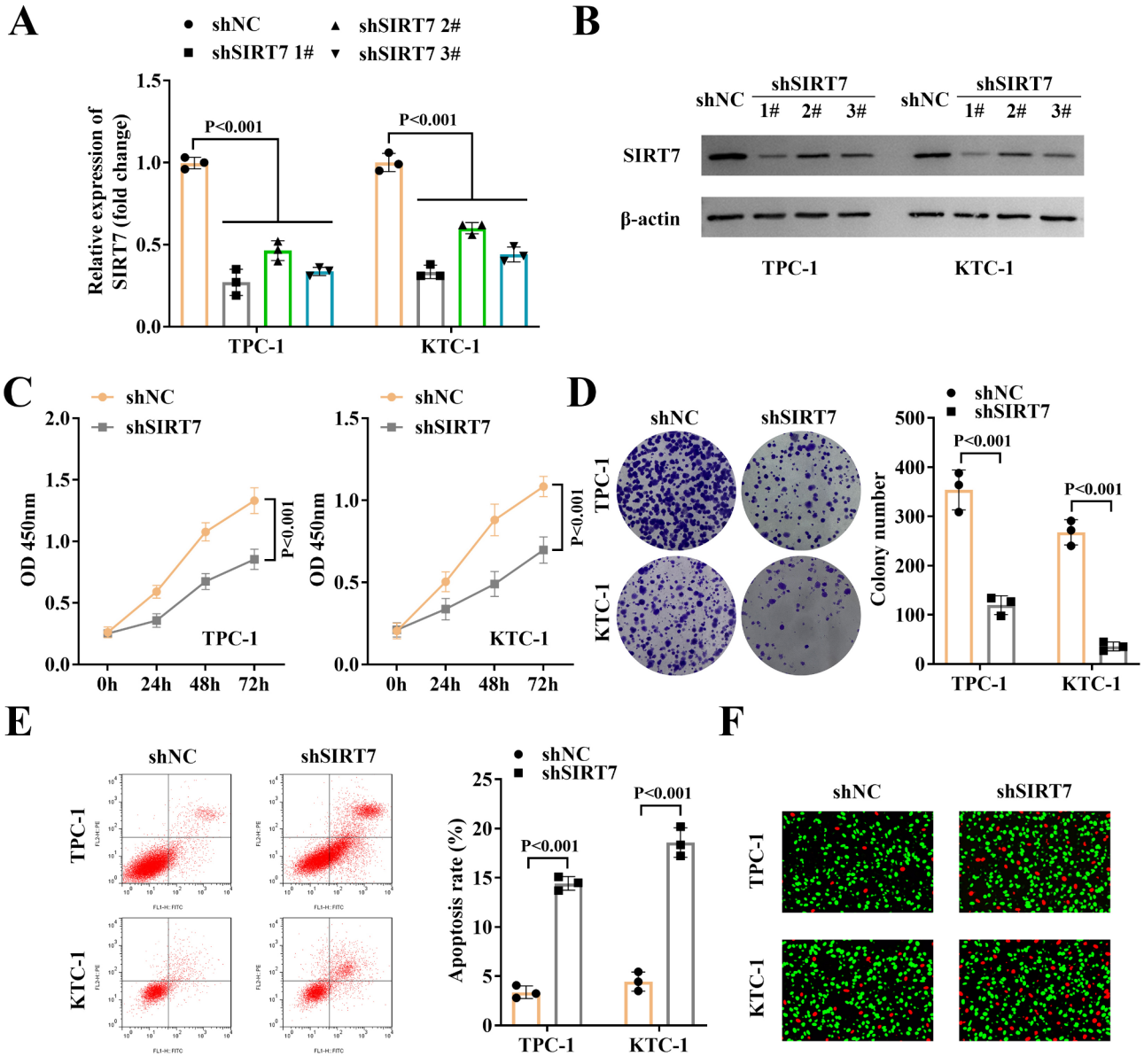

Fig. 2 Silencing of SIRT7 inhibits apoptosis in PTC. (**A-B**) After shNC and three different shSIRT7 transfection, the expression of SIRT7 was measured using qPCR and western blot. (**C-D**) CCK-8 and colony formation experiments were used to analyze cell proliferation. (**E**) The apoptosis rate of PTC cells was detected with flow cytometry. (**F**) Calcein AM (CA) and Propidium Iodide (PI) co-staining images of PTC cells with various treatments. All data are expressed as the means ± SD. ($n = 3$ independent experiments)

sites (K6, K589, and K652) with the highest possibility were predicted in LATS1 at the GPSuc website and were selected for subsequent confirmation (Fig. 3J). Compared with WT-LATS1, the expression and the succinylation levels of LATS1 were downregulated when K589 site was mutated in TPC-1 cells (Fig. 3K). LATS1 levels were more stable after SIRT7 knockdown than shNC in TPC-1 cells (Fig. 3L). Based on the above data, we concluded that SIRT7 regulates LATS1 by succinylation modification.

Silencing of LATS1 abolishes the Inhibition of proliferation and the promotion of apoptosis of PTC cells by SIRT7 knockdown

Subsequently, this study continued to investigate the effect of LATS1 on PTC cells. For functional detection, LATS1 expression was suppressed when three different shRNA interference sequences targeting the LATS1 gene were transfected into TPC-1 and KTC-1 cells compared to the shNC group (Fig. 4A and B). The viability of PTC cells was inhibited by silencing of SIRT7 and then restored after co-transfecting with shLATS1 (Fig. 4C). Likewise, according to data from colony formation

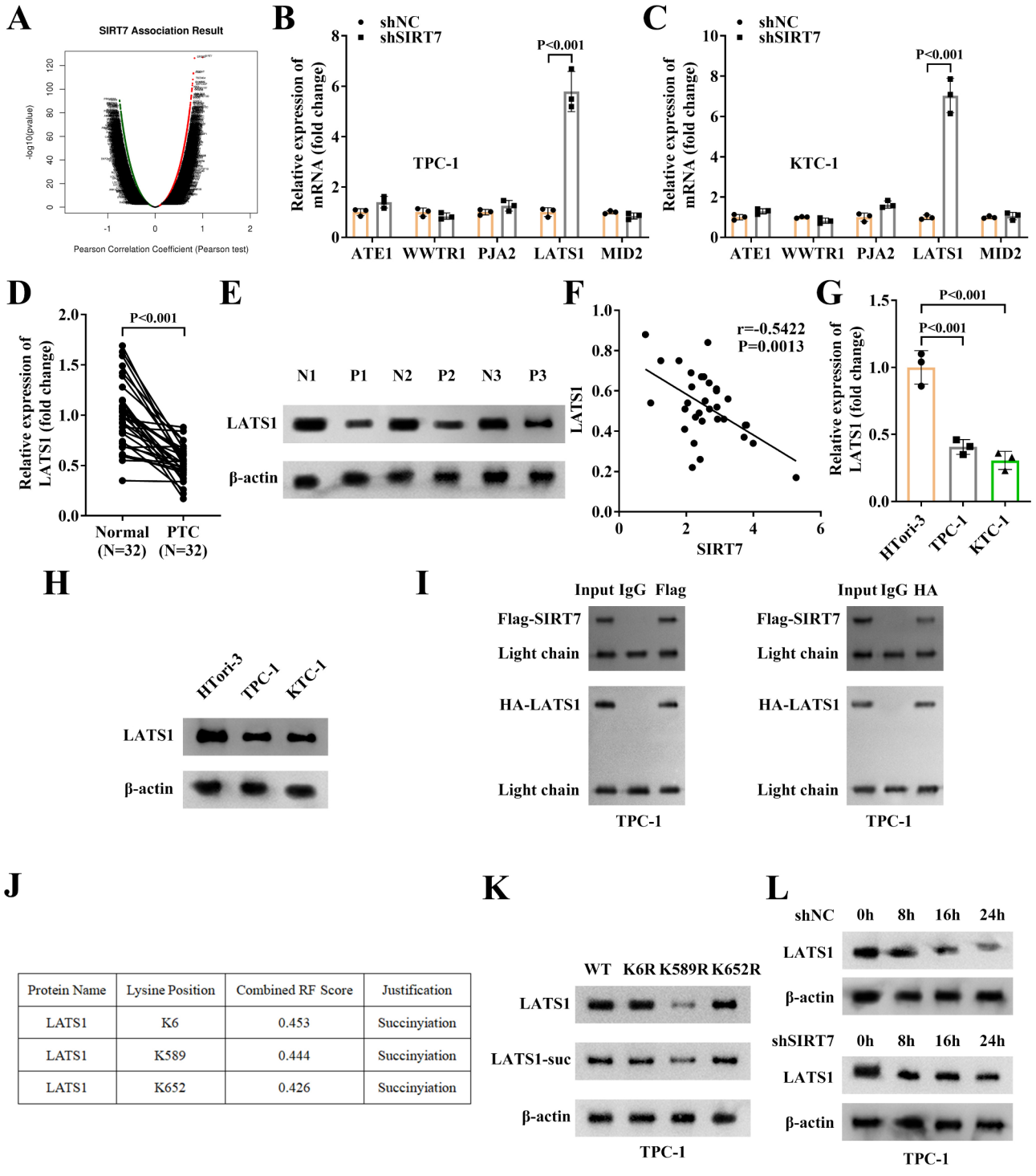

Protein Name	Lysine Position	Combined RF Score	Justification
LATS1	K6	0.453	Succinyiation
LATS1	K589	0.444	Succinyiation
LATS1	K652	0.426	Succinyiation

Fig. 3 SIRT7 regulates LATS1 by succinylation modification. (**A**) Possible targets of SIRT7 were predicted using online databases (LinkedOmics Suite). (**B-C**) The expression of genes associated with SIRT7 was analyzed using qPCR. (**D**) LATS1 expression in PTC ($n = 32$) and normal para-cancerous ($n = 32$) tissues was measured using qPCR. (**E**) The protein expression of LATS1 was measured by western blot. (**F**) Pearson correlation coefficient was used to analyze the correlation between SIRT7 and LATS1 in tumor tissues. (**G-H**) q-PCR and western blot were performed to evaluate the expression of LATS1 in normal thyroid cell lines Nthyori-3 and PTC cell lines (TPC-1 and KTC-1). (**I**) Co-IP was performed to detect the interaction of SIRT7 with LATS1 in TPC-1 cells. (**J**) LATS1 succinylation sites were predicted by the GPSuc website. (**K**) Western blot was used to evaluate the effect of LATS1 K6R, K589R, and K652R on the succinylation and protein levels of LATS1. (**L**) Western blot was used to evaluate the effects of SIRT7 knockdown on the LATS1 stability after 0, 8, 16, and 24 h of incubation with cycloheximide in TPC-1 cells. All data are expressed as the means ± SD. ($n = 3$ independent experiments)

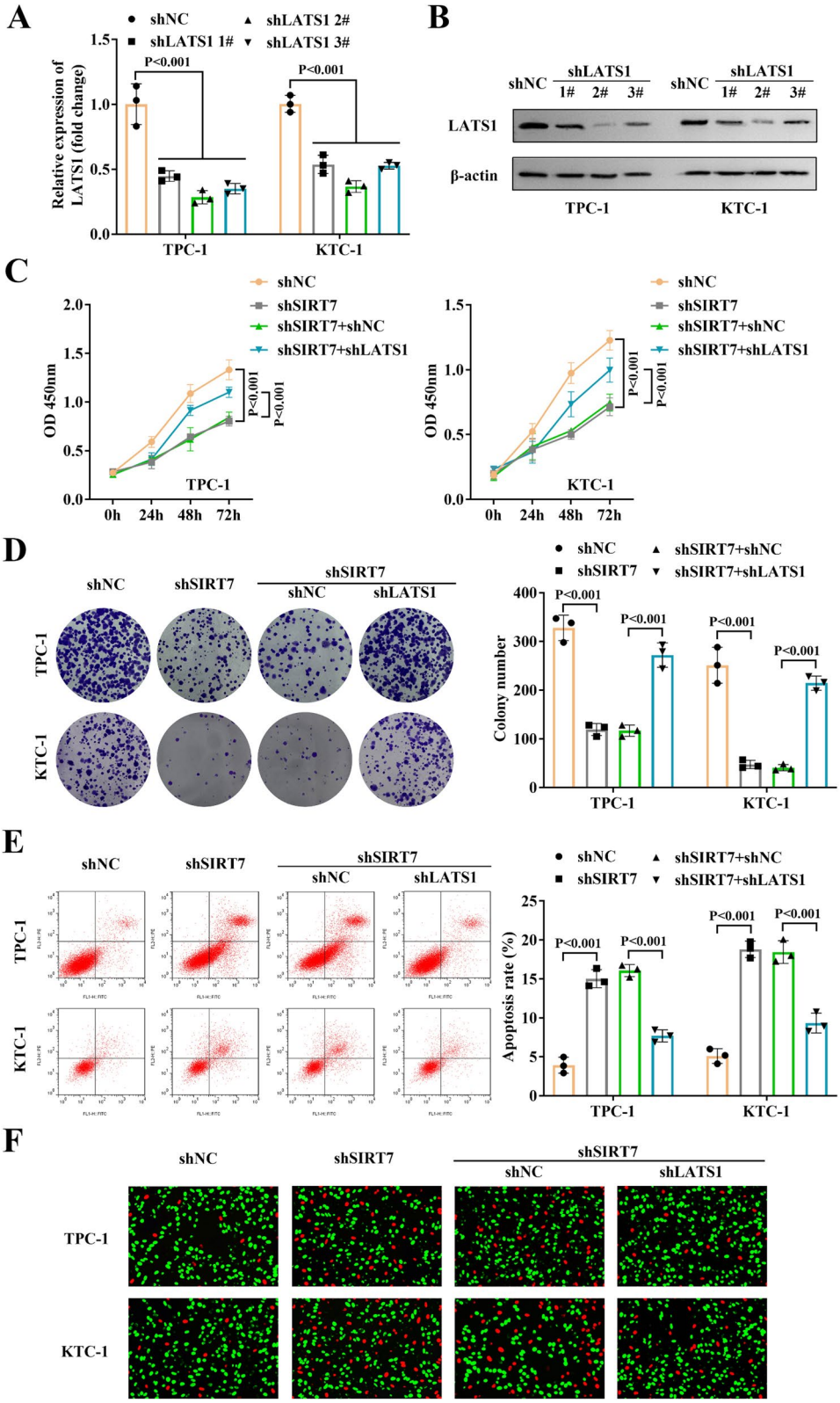

Fig. 4 Silencing of LATS1 abolishes the effects of SIRT7 knockdown on PTC cells. (**A-B**) After shNC and three different shLATS1 transfection, the expression of LATS1 was measured using qPCR and western blot. (**C-D**) CCK-8 and colony formation experiments were used to analyze cell proliferation. (**E**) The apoptosis rate of PTC cells was detected with flow cytometry. (**F**) Calcein AM (CA) and Propidium Iodide (PI) co-staining images of PTC cells with various treatments. All data are expressed as the means ± SD. ($n = 3$ independent experiments)

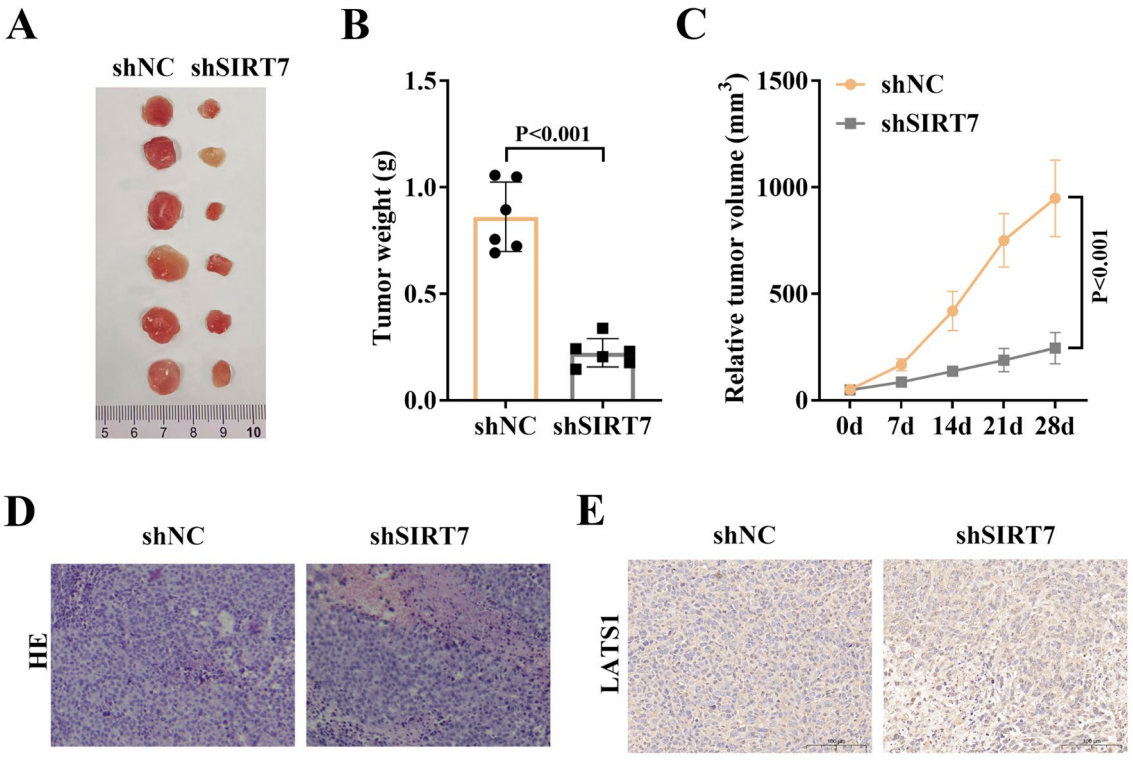

Fig. 5 Silencing SIRT7 inhibits tumor growth in mice. (**A-C**) The size, weight, and volume of tumor in sh-SIRT7 and sh-NC groups. (**D**) HE staining assay was performed to assess tumor pathophysiology in the sh-SIRT7 and sh-NC groups. (**E**) IHC assay assessed LATS1 protein levels in the sh-SIRT7 and sh-NC groups. All data are expressed as the means ± SD. (*n* = 6 independent experiments)

analysis, repressing LATS1 abolished the inhibition of colonies triggered by SIRT7 silencing (Fig. 4D). The apoptosis of TPC-1 and KTC-1 cells was increased by SIRT7 knockdown, which was recovered by LATS1 silencing (Figure E and F). These observations indicated that silencing of LATS1 abolishes the effects of SIRT7 knockdown on PTC cells.

SIRT7 promotes tumor growth in vivo

Finally, we evaluated the effect of SIRT7 on tumorigenic capacity in nude mice. The size and average weight in the SIRT7 silencing group were significantly decreased compared to the shNC group (Fig. 5A and B). Additionally, inhibiting SIRT7 expression significantly suppressed tumor growth compared with the shNC group (Fig. 5C). Meanwhile, HE pathological staining results show that compared with the control group, tumor tissues of mice in the shSIRT7 group had slight necrosis and a small amount of cell infiltration. (Fig. 5D). To further validate the regulatory effect of SIRT7 on LATS1 in vivo, an IHC assay was performed in the sections of the above xenograft tumors using the corresponding antibodies. The results indicated that LATS1 expression was significantly upregulated in the SIRT7 silencing tumors relative to the shNC group (Fig. 5E). Given the above observations, we concluded that SIRT7 promotes tumor growth in vivo.

Discussion

PTC is a multifactorial disease, the incidence of which increases year by year. Aggressive PTC with local or distant metastasis, structural recurrence, and even progression to high-grade cancer can be life-threatening, which poses a serious public health challenge to society [20]. Therefore, exploring the potential molecular mechanism of PTC is of great significance for discovering new therapeutic targets.

SIRT7 has been shown to play an important role in carcinogenesis, accelerating the development and progression of several tumors. For example, SIRT7 promotes abnormal activation of YAP in the Hippo pathway and proliferation of cancer cells in hepatocellular carcinoma via suppressing MST1 [21]. SIRT7 facilitates the development of ovarian cancer by suppressing GATA4 and activating the Wnt signaling pathway [22]. Besides, SIRT7 promotes autophagy and inhibits oxidative stress in cervical squamous cell carcinoma cells by regulating the USP39/FOXM1 axis [23]. However, our current understanding of the biological function of SIRT7 in PTC is still very limited. A previous study has indicated that SIRT7 expression is upregulated in PTC and demonstrates that SIRT7 knockdown significantly inhibits the proliferation and colony formation and induces cycle arrest and apoptosis of TC cells [16]. Consistent with this finding,

we also confirmed that SIRT7 expression was elevated in PTC tissues and two PTC cell lines. Interestingly, subsequent functional experiments showed that silencing of SIRT7 could inhibit the proliferation and promote the apoptosis of PTC cells, suggesting that SIRT7 has a protumor effect in PTC.

Succinylation, which is regulated by SIRT7, has been implicated in the onset and development of cancer. SIRT7 catalyzes the desuccinylation of protein arginine methyltransferase 5 to participate in lipid reprogramming and promote tumor growth and metastasis [24]. Succinate dehydrogenase (SDH) participates in the regulation process of succinylation. In PTC and follicular carcinoma cell lines, the SDH subunit impaired the function of PTEN, which resulted in the inhibition of apoptosis and the promotion of the migration of TC cells [25]. Thyroglobulin (TG) is used as a potential biomarker for the diagnosis of TC, which can predict tumor recurrence and metastasis [26]. Extensive succinylation can induce cleavage of 12 S TG and thereby affect the synthesis of thyroxine [27]. In a previous study, SIRT7 promotes the proliferation and migration of TC cells by regulating the desuccinylation of KIF23 [15]. Therefore, we attempted to investigate the effect of SIRT7 on protein succinylation in PTC. We found that SIRT7 directly bound to LATS1 and negatively regulated LATS1 expression. In addition, silencing of SIRT7 enhanced the stability of LATS1 protein by suppressing the desuccinylation at K589 site. It is suggested that LATS1 may be involved in the development of PTC.

As a tumor suppressor, LATS1 is involved in the progression of many types of cancer, including PTC. It has been found that the overexpression of LINC01186 inhibits the proliferation and invasion of TPC-1 cells via increasing the expression of LATS1 [28]. In addition, the upregulation of STK4 can increase the expression of LATS1, which inhibits the proliferation of TC cells and promotes apoptosis and autophagy through the hippo signaling pathway [29]. In the present study, the expression of LATS1 was decreased in PTC tissues and two PTC cell lines. Of note, silencing LATS1 can eliminate the inhibitory effect on PTC cell proliferation and induction of apoptosis caused by SIRT7 knockdown. These results suggest that the silencing of SIRT7 inhibits the carcinogenesis of PTC by promoting the succinylation of LATS1. Finally, we established a mouse xenograft tumor model to further investigate the role of SIRT7 in vivo. The results showed that silencing of SIRT7 inhibited tumor growth in mice and increased LATS1 protein levels, suggesting that silencing SIRT7 inhibits tumor growth by upregulating LATS1 expression.

The limitations of this study are the insufficient number and diversity of clinical samples used. The specific molecular mechanism of how SIRT7 precisely regulates the succinylation level of LATS1, including the enzymes or factors involved, still needs to be further explored. The study did not address specific effector molecules or signaling pathways downstream of the SIRT7-LATS1 axis, which limits the full understanding of the mechanism of action of SIRT7. Overall, these limitations do not affect the importance and innovation of this study, but provide a clear direction and room for improvement for future research.

In conclusion, in this study, the tumor-supporting role and underlying mechanisms of SIRT7 were characterized in PTC. SIRT7 interacts with LATS1, and silencing of SIRT7 promotes the expression and succinylation modification of LATS1, which can inhibit tumor cell proliferation and induce apoptosis, thereby slowing down the progression of PTC. This study may provide a possible strategy and target for the treatment of PTC.

Supplementary Information

The online version contains supplementary material available at https://doi.org/10.1186/s12885-025-13779-9.

Supplementary Material 1

Acknowledgements

Not applicable.

Author contributions

All authors participated in the design, interpretation of the studies and analysis of the data and review of the manuscript. Q L drafted the work and revised it critically for important intellectual content and was responsible for the acquisition, analysis and interpretation of data for the work; G P made substantial contributions to the conception or design of the work. All authors read and approved the final manuscript.

Funding

The work was supported by Scientific Research Project of Jilin Provincial Education Department under grant number JJKH20250819KJ.

Data availability

The datasets used and/or analysed during the current study are available from the corresponding author on reasonable request.

Declarations

Ethics approval and consent to participate

This study was approved by the Ethics Committee of Affiliated Hospital of Beihua University. This study was performed in line with the principles of the Declaration of Helsinki. Informed consent was obtained from all individual participants included in the study. All animal experiments should comply with the ARRIVE guidelines. All methods were carried out in accordance with relevant guidelines and regulations.

Consent for publication

Not applicable.

Competing interests

The authors declare no competing interests.

Received: 30 August 2024 / Accepted: 20 February 2025
Published online: 06 March 2025

References

1. Basolo F, Macerola E, Poma AM, Torregrossa L. The 5(th) edition of WHO classification of tumors of endocrine organs: changes in the diagnosis of follicular-derived thyroid carcinoma. Endocrine. 2023;80:470–6.
2. Zhang X, Chen W, Fang Q, Fan J, Feng L, Guo L, et al. Corrigendum: lateral lymph node metastases in T1a papillary thyroid carcinoma: stratification by tumor location and size. Front Endocrinol (Lausanne). 2022;13:852751.
3. Coca-Pelaz A, Shah JP, Hernandez-Prera JC, Ghossein RA, Rodrigo JP, Hartl DM, et al. Papillary thyroid Cancer-Aggressive variants and impact on management: A narrative review. Adv Ther. 2020;37:3112–28.
4. Zhao Y, Zhang Z, Tan M, Xie Z, Dai L, Chen Y. Identification of lysine succinylation as a new post-translational modification. Nat Chem Biol. 2011;7:58–63.
5. Dai X, Zhou Y, Han F, Li J. Succinylation and redox status in cancer cells. Front Oncol. 2022;12:1081712.
6. Alleyn M, Breitzig M, Lockey R, Kolliputi N. The dawn of succinylation: a post-translational modification. Am J Physiology: Cell Physiol. 2018;314:C228–32.
7. Chen XF, Tian MX, Sun RQ, Zhang ML, Zhou LS, Jin L et al. SIRT5 inhibits peroxisomal ACOX1 to prevent oxidative damage and is downregulated in liver cancer. EMBO Rep 2018;19.
8. Wang C, Zhang C, Li X, Shen J, Xu Y, Shi H, et al. CPT1A-mediated succinylation of S100A10 increases human gastric cancer invasion. J Cell Mol Med. 2019;23:293–305.
9. Bringman-Rodenbarger LR, Guo AH, Lyssiotis CA, Lombard DB. Emerging roles for SIRT5 in metabolism and Cancer. Antioxid Redox Signal. 2018;28:677–90.
10. Lu K, Han D. A review of the mechanism of succinylation in cancer. Med (Baltim). 2022;101:e31493.
11. Mu R, Ma Z, Lu C, Wang H, Cheng X, Tuo B, et al. Role of succinylation modification in thyroid cancer and breast cancer. Am J Cancer Res. 2021;11:4683–99.
12. Tang M, Tang H, Tu B, Zhu W. SIRT7: a Sentinel of genome stability. Open Biol. 2021;11:210047.
13. Raza U, Tang X, Liu Z, Liu B. SIRT7: the seventh key to unlocking the mystery of aging. Physiol Rev. 2024;104:253–80.
14. Lagunas-Rangel FA. The dark side of SIRT7. Mol Cell Biochem 2023.
15. Wu Y, Chen W, Miao H, Xu T. SIRT7 promotes the proliferation and migration of anaplastic thyroid cancer cells by regulating the desuccinylation of KIF23. BMC Cancer. 2024;24:210.
16. Li H, Tian Z, Qu Y, Yang Q, Guan H, Shi B, et al. SIRT7 promotes thyroid tumorigenesis through phosphorylation and activation of Akt and p70S6K1 via DBC1/SIRT1 axis. Oncogene. 2019;38:345–59.
17. Furth N, Aylon Y. The LATS1 and LATS2 tumor suppressors: beyond the Hippo pathway. Cell Death Differ. 2017;24:1488–501.
18. Zhang ML, Sun WH, Wu HQ, Liu ZD, Wang P. Knockdown of microRNA-103a-3p inhibits the malignancy of thyroid cancer cells through Hippo signaling pathway by upregulating LATS1. Neoplasma. 2020;67:1266–78.
19. Mo Y, Lin R, Liu P, Tan M, Xiong Y, Guan KL, et al. SIRT7 deacetylates DDB1 and suppresses the activity of the CRL4 E3 ligase complexes. FEBS J. 2017;284:3619–36.
20. McLeod D, Zhang L, Durante C, Cooper DS. Contemporary debates in adult papillary thyroid Cancer management. Endocr Rev. 2019;40:1481–99.
21. Gu Y, Ding C, Yu T, Liu B, Tang W, Wang Z, et al. SIRT7 promotes Hippo/YAP activation and cancer cell proliferation in hepatocellular carcinoma via suppressing MST1. Cancer Sci. 2024;115:1209–23.
22. Li G, Xu W, Li X, Chen M, Shi Y, Wei M, et al. Oncogenic SIRT7 inhibits GATA4 transcriptional activity and activates the Wnt signaling pathway in ovarian cancer. Gynecol Oncol. 2023;171:39–48.
23. Yu J, Yuan S, Song J, Yu S. USP39 interacts with SIRT7 to promote cervical squamous cell carcinoma by modulating autophagy and oxidative stress via FOXM1. J Transl Med. 2023;21:1–807.
24. Yuan HF, Zhao M, Zhao LN, Yun HL, Yang G, Geng Y, et al. PRMT5 confers lipid metabolism reprogramming, tumour growth and metastasis depending on the SIRT7-mediated desuccinylation of PRMT5 K387 in tumours. Acta Pharmacol Sin. 2022;43:2373–85.
25. Yu W, He X, Ni Y, Ngeow J, Eng C. Cowden syndrome-associated germline SDHD variants alter PTEN nuclear translocation through SRC-induced PTEN oxidation. Hum Mol Genet. 2015;24:142–53.
26. Valenta LJ, Michel Béchet M. Ultrastructure and biochemistry of thyroid carcinoma. Cancer. 1977;40:284–300.
27. Shifrin S, Kohn LD. Binding of thyroglobulin to bovine thyroid membranes. Role of specific amino acids in receptor recognition. J Biol Chem. 1981;256:10600–5.
28. Wang N, Duan H, Zhang C, Zhou Y, Gao R. The LINC01186 suppresses cell proliferation and invasion ability in papillary thyroid carcinoma. Oncol Lett. 2018;16:5639–44.
29. Yang LX, Wu J, Guo ML, Zhang Y, Ma SG. Suppression of long non-coding RNA TNRC6C-AS1 protects against thyroid carcinoma through DNA demethylation of STK4 via the Hippo signalling pathway. Cell Prolif. 2019;52:e12564.

Publisher's note